

## Article

# Continuous Glucose Monitoring in Hypoxic Environments Based on Water Splitting-Assisted Electrocatalysis

Lanjie Lei, Chengtao Xu, Xing Dong, Biao Ma <sup>\*</sup>, Yichen Chen, Qing Hao, Chao Zhao <sup>\*</sup> and Hong Liu <sup>\*</sup>

State Key Laboratory of Bioelectronics, School of Biological Science and Medical Engineering, Southeast University, Nanjing 210096, China

<sup>\*</sup> Correspondence: biao.ma@seu.edu.cn (B.M.); czhao86@seu.edu.cn (C.Z.); liuh@seu.edu.cn (H.L.)

**Abstract:** Conventional enzyme-based continuous glucose sensors in interstitial fluid usually rely on dissolved oxygen as the electron-transfer mediator to bring electrons from oxidase to electrode while generating hydrogen peroxide. This may lead to several problems. First, the sensor may provide biased detection results owing to fluctuation of oxygen in interstitial fluid. Second, the polymer coatings that regulate the glucose/oxygen ratio can affect the dynamic response of the sensor. Third, the glucose oxidation reaction continuously produces corrosive hydrogen peroxide, which may compromise the long-term stability of the sensor. Here, we introduce an oxygen-independent nonenzymatic glucose sensor based on water splitting-assisted electrocatalysis for continuous glucose monitoring. For the water splitting reaction (i.e., hydrogen evolution reaction), a negative pretreatment potential is applied to produce a localized alkaline condition at the surface of the working electrode for subsequent nonenzymatic electrocatalytic oxidation of glucose. The reaction process does not require the participation of oxygen; therefore, the problems caused by oxygen can be avoided. The nonenzymatic sensor exhibits acceptable sensitivity, reliability, and biocompatibility for continuous glucose monitoring in hypoxic environments, as shown by the in vitro and in vivo measurements. Therefore, we believe that it is a promising technique for continuous glucose monitoring, especially for clinically hypoxic patients.



**Citation:** Lei, L.; Xu, C.; Dong, X.; Ma, B.; Chen, Y.; Hao, Q.; Zhao, C.; Liu, H. Continuous Glucose Monitoring in Hypoxic Environments Based on Water Splitting-Assisted Electrocatalysis. *Chemosensors* **2023**, *11*, 149. <https://doi.org/10.3390/chemosensors11020149>

Academic Editors: Xiaobing Zhang, Lin Yuan and Guoliang Ke

Received: 28 December 2022

Revised: 6 February 2023

Accepted: 16 February 2023

Published: 18 February 2023



**Copyright:** © 2023 by the authors. Licensee MDPI, Basel, Switzerland. This article is an open access article distributed under the terms and conditions of the Creative Commons Attribution (CC BY) license (<https://creativecommons.org/licenses/by/4.0/>).

**Keywords:** nonenzymatic; glucose; sensor; interstitial fluid; hypoxia

## 1. Introduction

Continuous glucose monitoring (CGM) is an effective tool for glucose management of diabetics [1,2]. CGM systems can provide continuous, real-time information on blood glucose level and even predict its future trend without frequent finger pricks [3,4]. With the CGM results as a timely feedback, one can adjust diets or dosage of insulin or other drugs to better regulate glycemic levels, which can avoid life-threatening hypoglycemia, hyperglycemia events, and diabetes-related complications [5,6]. Several CGM systems have been designed and optimized for usage by diabetics, which have a population of almost half billion worldwide, leading to a huge market.

To date, the most popular detection reaction for the CGM system is glucose oxidation by oxygen that is catalyzed by glucose-oxidase (GOx) due to its compatibility with long-time glucose monitoring [2,7]. Therefore, the CGM detection relies on dissolved oxygen in interstitial fluid (ISF) as the electron-transfer mediator to bring electrons from oxidase to electrode [2,8]. This kind of oxygen-dependent sensor may lead to biased results due to the fluctuation of oxygen in tissues. Specifically, under hypoxic circumstances caused by various pathological mechanisms, the application of conventional CGM can be highly constrained.

For example, acute respiratory distress syndrome (ARDS) caused by COVID-19 infection can lead to tissue hypoxia [9]. During the infection, the antiviral immunity and inflammatory reaction can change insulin sensitivity, which leads to aggravation of impaired glucose metabolism [10]. Some clinical medications, such as corticosteroid dexamethasone or other antiviral agents, may cause hyperglycemia when used for the treatment

of COVID-19 patients [9,11,12]. Anemia (e.g.,  $\beta$ -thalassemia) may result in a significant reduction in oxygen delivery to tissue, leading to tissue hypoxia [13–15]. The patients with impaired glucose tolerance also require CGM for glucose management [14,16]. In addition, it is widely known that solid tumors exhibit hypoxic and/or anoxic tissue areas, which is accompanied by increased glucose uptake and metabolism (the Warburg effect) [17]. Therefore, the conventional oxygen-dependent glucose sensors may not be suitable for the above hypoxic circumstances. Moreover, the glucose oxidation reaction continuously produces corrosive hydrogen peroxide once implanted, which compromises long-time stability of the sensor [18]. Furthermore, because concentration of the dissolved oxygen is significantly lower than glucose concentration in ISF, a polymer membrane is often required to maintain a slow mass transfer of glucose to the electrode, which can complicate the dynamic response of the sensor [7,19]. The failure of the polymer membrane, for example due to hydrogen peroxide, can also restrict the working time of the implanted sensor. Therefore, a development of CGM that does not rely on the oxygen-based reaction is highly required.

In contrast to the first-generation glucose sensor based on oxygen, some CGM sensors are based on second-generation glucose sensing strategy. One example is “wired” enzyme technology for in vivo glucose measurement, which connects enzymes to the electrode surface via cross-linked redox-conductive polymer ‘wires’, enables continuous glucose monitoring, and reduces sensitivity to changes in oxygen concentration in vivo [1,20]. However, as the CGM sensors are also based on enzymes, it remains vulnerable to changes in the environment and enzyme activity [21]. In this work, we report a nonenzymatic CGM sensor based on water splitting-assisted electrocatalysis (WSE) for hypoxic environments. Specifically, the hydrogen evolution reaction, which is part of the water splitting reaction [22–24], is employed to produce hydroxide ions via a negative potential pretreatment on the Au electrode, which can create the necessary alkaline pH conditions for the electrocatalytic oxidation of glucose. Subsequently, a potential for glucose detection is applied, and the anodic current is measured. Finally, a positive potential is applied to clean and regenerate the electrode for the next test, which is beneficial for long-term repeated tests. The sensor is tested by in vitro experiments for glucose determination, and its biocompatibility is also characterized. It is worth noting that neither the water splitting reaction nor the glucose oxidation require oxygen, so the sensor will not be affected by the problems from the oxygen deficiency. Finally, the WSE-based glucose sensor is used for CGM in hypoxic environment (Figure 1), including systemic hypoxic rat and tumor-bearing mice.

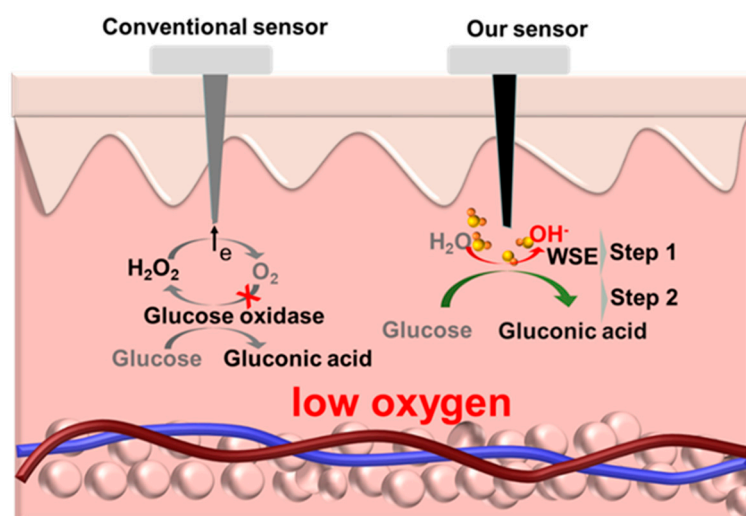


**Figure 1.** Schematic illustration of a conventional CGM sensor and our sensor for ISF glucose monitoring under hypoxic microenvironment. For the conventional glucose sensor shown on the left, the detection reaction relies on oxygen, which cannot work properly in hypoxic environment. However, for our sensor shown on the right, the detection reaction requires no oxygen.

## 2. Materials and Methods

### 2.1. Materials

Chemicals, including D(+)-glucose, ethanol, saccharose, acetone, phenylcarbinol, ascorbic acid (AA), acetaminophen (AP),  $\text{NaH}_2\text{PO}_4$ ,  $\text{Na}_2\text{HPO}_4$ , NaCl, KCl,  $\text{GaCl}_2$ ,  $\text{MgSO}_4$ , uric acid (UA), and 5% Nafion, were bought from Sigma (Shanghai, China). Calcein-AM/PI Double Stain Kit was purchased from Beyotime Biotechnology (Nanjing, China). Streptozotocin was bought from Yeasen (Shanghai, China). Insulin and Cell Counting Kit-8 (CCK-8) was purchased from Sanofi (Beijing, China). 4-(2-hydroxyethyl) piperazine-1-ethane sulfonic acid (HEPES) was purchased from Aladdin (Shanghai, China). Tumor necrosis factor- $\alpha$  (TNF- $\alpha$ ) and interleukin-6 (IL-6) were obtained from Thermo Fisher (Shanghai, China). Tecoflex SG-85A polyurethane (PU) was obtained from Thermedics (Shanghai, China). Mouse embryonic fibroblast cell line (NIH-3T3) and human bladder transitional cell cancer cell line (T24) cells were obtained from the Cell Bank of the Chinese Academy of Sciences (Shanghai, China). Glass capillary with three parallel tubes (0.6 mm inner diameter), Au (99.9%, 0.2 mm diameter), Ag (99.9%, 0.2 mm diameter), and Pt (99.9%, 0.2 mm diameter), were obtained from Alfa Aesar (Shanghai, China). Artificial ISF with pH 7 was composed of NaCl, HEPES,  $\text{CaCl}_2$ , KCl,  $\text{MgSO}_4$ ,  $\text{NaH}_2\text{PO}_4$ , saccharose, and D(+)-glucose according to previous literature [25]. Phosphate buffer saline with different pH were composed of  $\text{NaH}_2\text{PO}_4$ ,  $\text{Na}_2\text{HPO}_4$ , NaCl, and KCl. Sprague Dawley (SD) rats (6 ~ 8 weeks old) and nude mice (4~6 weeks old, male) were purchased from Qinglongshan Animal Farm (Nanjing, China). All animal experiments were carried out according to National Institutes of Health Guide for the Care and Use of Laboratory Animals and were approved by the Scientific Ethical Committee of the School of Biological Sciences and Medical Engineering of Southeast University.

### 2.2. Sensor Fabrication

The nonenzymatic glucose sensing device was composed of an Au working electrode, a Pt counter electrode, and an Ag/AgCl reference electrode, which were assembled in the stretched glass capillary (Figure S1). The Ag/AgCl reference electrode was prepared by chlorination of the Ag wire based on a constant current method [26]. To prevent interference and improve biocompatibility, the surface of the electrodes was coated with Nafion and then 5% PU (*w/w*), as previously reported [26].

### 2.3. In Vitro Glucose Detection

For the glucose detection, a potential of  $-2.0$  V was first applied to the working electrode to create an alkaline pH condition by the hydrogen evolution reaction. Subsequently, a potential of  $0.20$  V was applied for glucose detection under the alkaline condition. Then, a potential of  $1.0$  V was applied to clean and regenerate the electrode, which was beneficial for long-term monitoring. The hypoxic artificial ISF was prepared by nitrogen purging.

### 2.4. In Vitro Cytotoxicity Tests

To test the cytotoxicity of the sensor, we conducted a direct contact cell culture toxicity test. The NIH-3T3 cells were seeded in 24-well plate with a density of  $6 \times 10^4$  cells/mL and cultured for 24 h. Then, the cells were divided into different groups. After coculture with the glass capillary tube, electrodes, and assembled sensor for 24 h, the cells in different groups were stained with Calcein-AM and PI. At the same time, the cytotoxicity was also evaluated using CCK-8. Specifically, the glass capillary tube, electrodes, and assembled sensor were immersed in 1.0 mL aliquots of cell culture medium for 48 h, respectively. Subsequently, the leaching liquors were used to prepare cell suspensions with a density of  $1 \times 10^5$  cells/mL, which were cultured in a 96-well plate for 48 h for cytotoxicity test by CCK-8.

### 2.5. *In Vivo* Biocompatibility Test

The normal skin tissue and the tissues implanted with the sensor were obtained for the biocompatibility test *in vivo*. The collected skin tissues were fixed in paraformaldehyde and then processed by dehydration, embedding, and paraffin sectioning. Finally, the skin tissues samples were stained to show the inflammation-related factors, including TNF- $\alpha$  and IL-6, which are the indicator of the biocompatibility of the implant.

### 2.6. Glucose Detection in Normal Rat

The rats were anesthetized and fixed on the operating plate. Then, the sensor was implanted into the subcutaneous tissue. Before the test, at least 20 min was required to obtain a stable current. For comparison, two commercial CGM systems were used for glucose monitoring. One sensor (CGM-1) is based on electron transfer of oxygen, which is the 1st-generation glucose sensor, and the other one (CGM-2) uses wired enzyme technology to avoid the use of oxygen as a mediator. A commercial finger-prick glucometer (Accu-Chek, Roche, Germany) was also used as the reference. For long-time glucose monitoring of a rat *in vivo*, fasting glucose values were measured every 2 days using our sensor and CGM-2.

### 2.7. Animal Models

Normal and diabetic rats were placed in an anoxic tank to induce systemic hypoxia. The tank was filled with a mixture of air and nitrogen, and the oxygen concentration was monitored by an oxygen meter and maintained at approximately 12%. To obtain the diabetic rats, a single-dose of 60 mg/kg streptozotocin was injected intraperitoneally into the rats after fasting for 12 h to induce the diabetes, which was validated by a blood glucose levels above 16 mM after one week [27]. Tumor-bearing nude mice were also used as the animal model of local hypoxia, since the tumor created a localized hypoxic microenvironment [28]. To obtain the tumor-bearing nude mice, T24 cells were diluted to approximately  $1 \times 10^7$  cells/mL, and 0.10 mL aliquot of the cell suspension was injected subcutaneously into the back of each nude mouse. After 2 weeks, when the average size of the tumors was 3 mm, the animal model of local hypoxia was established.

## 3. Results and Discussion

### 3.1. Electrochemical Performance of the Sensor *In Vitro*

For the electrochemical oxidation of glucose at Au electrode, we introduced WSE on the Au electrode to produce hydroxide ions via a  $-2.0$  V potential pretreatment, which can create the necessary alkaline pH conditions. The pH near the pretreated Au electrode surface was measured by chronopotentiometry in PBS with a different pH to the previous reports [29]. The potential measured was linearly correlated to the pH of the solution (Figure S2a,b). After 20 s of pretreatment, the pH of the solutions was about 11 (Figure S2c). The electrochemical behavior of the nonenzymatic glucose sensor in the artificial ISF (pH 7.0) was investigated. We compared the cyclic voltammogram curves of Au electrode with and without pretreatment in the presence and absence of glucose solutions. The results in Figure 2a show that the current of the pretreated Au electrodes in glucose solutions increased significantly and the oxidation peak of glucose was about 0.2 V, which agreed with what we have previously reported [30]. It is well known that glucose is more active toward oxidation reaction under an alkaline condition, the pretreatment electrochemical reaction at  $-2.0$  V, which produced hydroxide via the hydrogen evolution reaction and served to create the necessary alkaline condition, assisting the subsequent electrochemical glucose oxidation.

For quantitative detection of glucose on the Au electrode, the dose-response curve was obtained in artificial ISF containing different concentrations of glucose, as shown in Figure 2b. The current increased with increasing glucose concentration, and a linear relationship between the current and glucose concentration was found (Figure 2b), with

correlation coefficient of 0.998. This suggested that the sensor can perform quantitative analysis of glucose concentration in hypoxia tissue fluid.

A common problem during glucose detection is the interference of other substances from the physiological samples. As shown in Figures 2c and S3, the electrode was highly selective towards glucose detection, as other species have a negligible effect on the detection results. This result was probably because the working electrode was coated with Nafion and PU, which served as a protection layer to reduce the interference. Furthermore, the repeatability and stability of the sensor were evaluated in artificial ISF 10 times. The replicated tests of the sensor indicated that the RSD was 3.33% (Figure S4). The stability of the sensor was assessed by testing the artificial ISF for 30 days and the RSD was 3.86% (Figure S5).

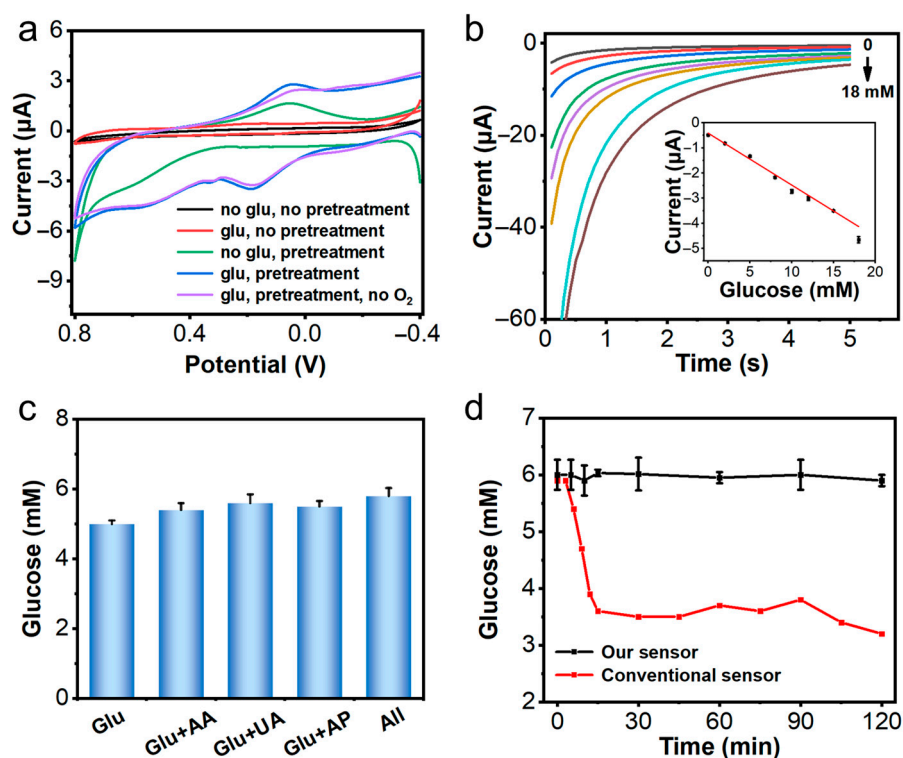


**Figure 2.** (a) Cyclic voltammogram in artificial ISF using the Au microelectrode with and without pretreatment. (b) Amperometric responses in artificial ISF with glucose. Insert: Current measured at 5 s. (c) Test results of artificial ISF containing 5.0 mM glucose and different interfering substances. (d) Glucose levels determined using our sensor and the enzyme sensor in hypoxic artificial ISF with 6.0 mM glucose.

Most commercialized implantable glucose sensors rely on the enzyme reaction, and the glucose concentration is usually determined by either monitoring O<sub>2</sub> consumption or H<sub>2</sub>O<sub>2</sub> production [8,31,32]. Hence, the detection signals of these sensors were highly influenced by the oxygen concentration, especially under hypoxic conditions. In comparison, for our sensor, the detection is based on the WSE reaction, which relies on no oxygen, so the fluctuation of dissolved oxygen would have a negligible influence on the glucose determination in principle. To demonstrate that, we compared the detection performance of our nonenzymatic sensor with that of the enzyme-based glucose sensor (CGM-1) in a hypoxic environment. We prepared a hypoxic artificial ISF sample by deoxidation based on nitrogen bubbling (Figure S6). The data indicated that as dissolved oxygen in the ISF decreased, the enzyme-based CGM-1 sensor led to biased results, while, for our sensor, the detection results were rather stable at different oxygen concentrations (Figure 2d). It demonstrated that our nonenzymatic sensor should be more suitable for glucose detection in hypoxic environments.

### 3.2. Cytotoxicity and Biocompatibility Test

The implanted sensor may have a negative effect on tissue or cause a serious immune response, which may compromise its long-term usage. To determine the cytotoxicity of the materials that we used for the electrochemical sensor, the NIH-3T3 cells were incubated in the presence of the glass capillary tube, electrode, and the sensor coated with Nafion and PU. After 24 h, the Calcein-AM/PI staining and CCK-8 were used for cell morphology, apoptosis, and viability assays. For Calcein-AM/PI staining, living cells can cleave Calcein-AM to calreticulin, generating green fluorescence, while apoptotic and necrotic cells take up PI into the nucleus, generating intense red fluorescence [33]. For the CCK-8 assay, the WST-8 dye label is reduced by dehydrogenases in the cells to form formazan, which is a water-soluble orange product. The amount of formazan dye produced by the cellular dehydrogenases correlates with the number of living cells [34]. Therefore, Calcein-AM/PI staining and CCK-8 are now routinely used to measure cell viability. It was found that the cells in all the groups showed normal attachment, spreading, and morphology characteristics, although certain apoptosis of cells were observed (Figure 3a). Moreover, the CCK-8 results showed that the cell viability was affected in different groups (Figure 3b). These results indicated that our sensor was of acceptable biocompatibility, which was highly required for *in vivo* tests. The immune response of our implanted sensor was also evaluated by immunohistochemical staining of TNF- $\alpha$  and IL-6, which are well known infectious inflammatory cytokines, as shown in Figure 3c. The results indicated that the expression of TNF- $\alpha$  and IL-6 in the enzyme sensors and our nonenzymatic sensor group were higher than the control group, but the expression of TNF- $\alpha$  (2.5 versus 2.2) and IL-6 (2.3 versus 1.9) was lower in our sensor than the conventional enzymatic sensor (Figure 3d). These results indicated that our sensor was of relatively higher biocompatibility and lower immune response.

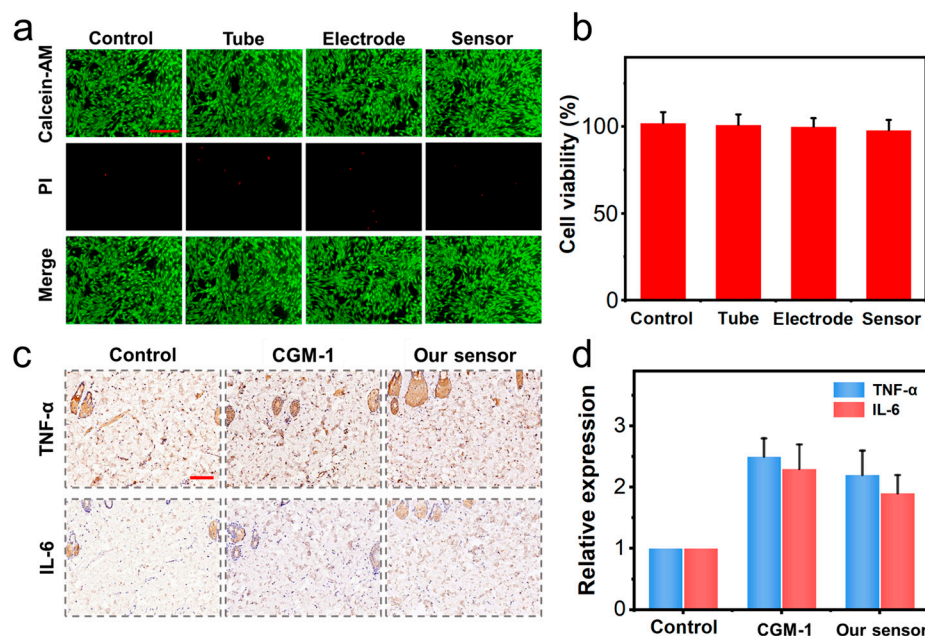


**Figure 3.** Fluorescent microscope images of (a) Calcein-AM and PI staining and (b) CCK-8 assays of NIH-3T3 cells. (c) Immunohistochemical staining and (d) relative expression levels of the TNF- $\alpha$  and IL-6 in control, CGM-1, and our nonenzymatic sensor groups. The red line in (a,c) represents the scale bar (100  $\mu$ m).

### 3.3. Glucose Detection in Normal Rat

We first analyzed glucose levels in a normal rat after injecting 0.40 mL of 4.0 mM glucose using our nonenzymatic glucose sensor and CGM-1, CGM-2 and Roche glucometer. CGM-1 sensor is based on first generation glucose biosensor technology. CGM-2 is based

on second generation glucose sensor, which use wired enzyme technology to avoid the use of oxygen as a mediator [32]. The Roche glucometer, a single test sensor, uses the glucose dehydrogenase-based amperometric test strips [35]. The results indicated that all sensors can work normally in normal (non-hypoxic) ISF microenvironment, and our nonenzymatic glucose sensor was generally correlated with the CGM-2 sensor (Figure 4a). A linear regression analysis resulted in a correlation equation:  $i (\mu\text{A}) = -0.01913 - 0.03507C (\text{mM})$  with a correlation coefficient of 0.947 (Figure 4b), which indicates that our nonenzymatic glucose sensor can be used for continuous monitoring of glucose in ISF. In addition, we also tested the performance of our sensor in long-time glucose monitoring in vivo. The results indicated that our sensors can work normally for more than 2 weeks, which was generally comparable with that attained using CGM-2 sensor (Figure S7).

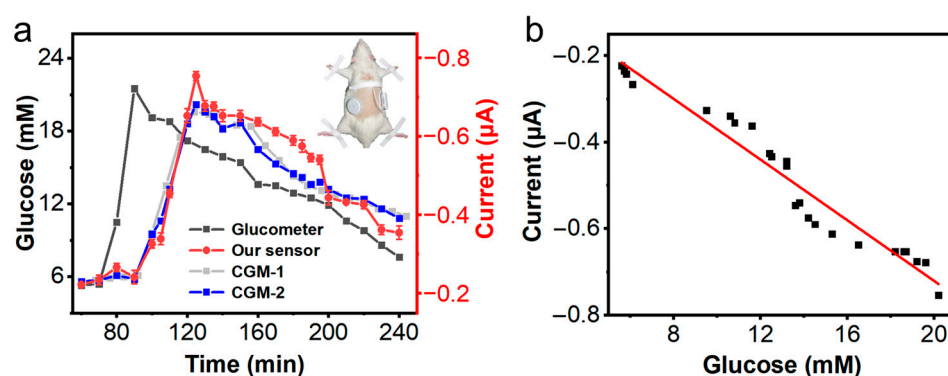


**Figure 4.** (a) Glucose detection using our sensor versus CGM-1 and CGM-2 sensor in a rat. Insert: A photograph of normal rat used for CGM. (b) Linear regression curves of current values measured by our nonenzymatic sensor and the glucose values measured by CGM-2.

### 3.4. Glucose Detection in Systemic Hypoxic Rat

To test the utility of our nonenzymatic glucose sensor under hypoxic microenvironment, we constructed two systematic hypoxia models in a normal rat and diabetic rat. The systemic hypoxic models in normal and diabetic rats were established by an anoxic tank as previously reported [36]. Nitrogen gas was slowly introduced into the anoxic tank with a rat to keep the  $\text{O}_2$  concentration monitored by the oxygen meter at 12%. The rat received hypoxia treatment for 4 h every day for hypoxic preconditioning to prevent lethal damage from occurring later [37]. On day 3 of hypoxia treatment, rats were anesthetized and placed in an anoxic tank for glucose monitoring (Figure 5d). The glucose levels in the systemic hypoxic models in normal and diabetic rats were analyzed using our glucose sensor and two commercial enzyme-based sensors (CGM-1 and CGM-2) and Roche glucometer.

As shown in Figure 5a, the current response of our glucose sensor generally correlated with glucometer and the correlation coefficient was 0.987. During hypoxia in normal rats, blood glucose levels gradually increased, which may be due to the altered glucose metabolism caused by the stress response [38]. The results showed that our nonenzymatic sensor had similar trends compared to the blood glucose values from glucometer, and the CGM-2 sensor showed a small decrease, while the CGM-1 sensor showed a large decrease (Figure 5b). For the systemic hypoxic model in diabetic rats, the results are shown in Figure 5c, the changes of glucose concentration measured by our nonenzymatic sensor were essentially the same as that measured by the glucometer. Before insulin (2.0 IU/kg) injection, CGM-1 assay results were lower than those measured by other sensors. After insulin injection, blood glucose concentration gradually decreased, but with the increase of hypoxia time, glucose concentration tended to increase, which may be a metabolic change caused by oxidative stress and hypoxia in diabetes mellitus [39]. However, the rise of glucose concentration measured by CGM-1 was low, and the rise of glucose concentration measured by CGM-2 was also lower than that of glucose concentration detected by glucometer and our glucose sensor. This may be attributed to the decreased

oxygen level in the ISF. Glucose dehydrogenase does not require oxygen for detection, so the glucose dehydrogenase-based amperometric test strips (Accu-Chek) were not affected by the decreased oxygen concentration [35]. The CGM-1 glucose sensor was susceptible to oxygen concentration fluctuation because of its oxygen dependence. The CGM-2 sensor employs a synthetic, polymeric redox-active mediator to replace oxygen, leading to little dependency on oxygen concentration in the ISF [19]. Although the CGM-2 sensor can partially address the oxygen problem, it still suffers from the variation of the environment and the enzyme activity [21].

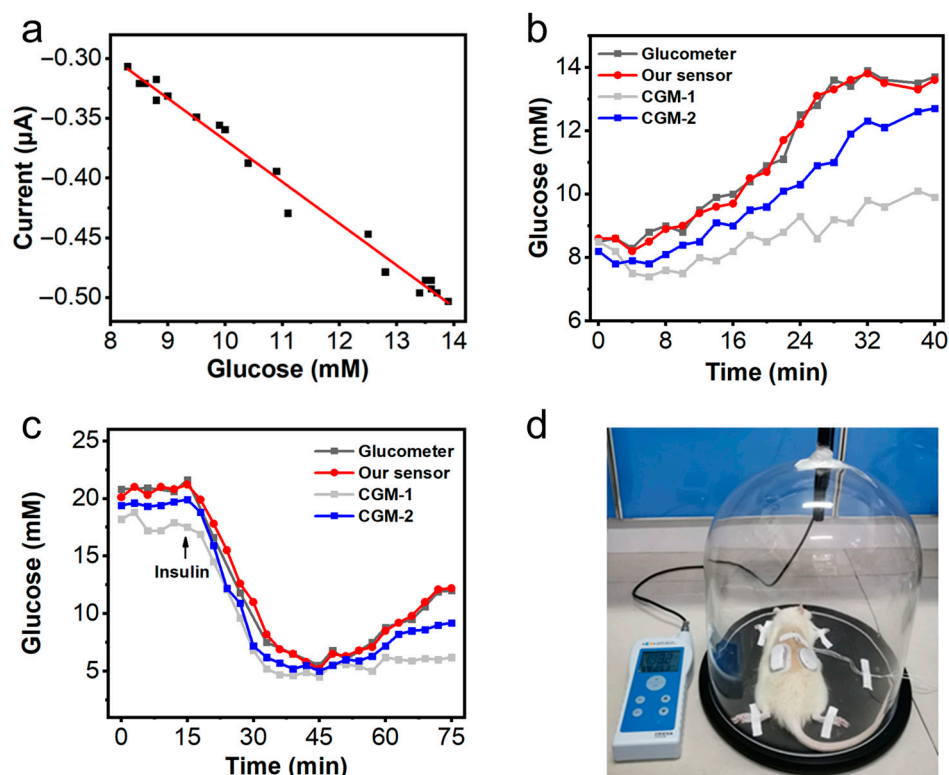


**Figure 5.** (a) A plot of the current measured from our sensor versus the blood glucose levels from glucometer. (b,c) Glucose values measured using our nonenzymatic sensor versus glucose values measured by the glucometer, CGM-1, and CGM-2 in systemic hypoxic models of (b) normal rat and (c) diabetic rat. (d) A photograph of the systemic hypoxic model for CGM.

### 3.5. Glucose Detection in Local Tissue Hypoxic Mice

To further test the reliability of our sensor in the local hypoxic microenvironment, we established a tumor-bearing mice model. In this experiment, our sensor was used to detect the glucose levels in the ISF surrounding the hypoxic microenvironment of tumor tissue in the tumor-bearing mice, and the blood glucose level was measured by the Roche glucometer as a reference. To detect ISF glucose during tumor growth, blood glucose values were measured every 2 weeks after mice were inoculated with tumor cells. Each test included three mice and experiments were repeated three times, and subsequently executed to measure the tumor size. The relationship between the growth of mouse tumor volume and the change of blood glucose is shown in Figure 6. The changes in glucose values measured by our sensor were consistent with the changes in blood glucose using Roche glucometer. This indicated that our nonenzymatic glucose sensor can be used for blood glucose detection in a local hypoxia model. Moreover, we found that the blood glucose appeared to be positively correlated with the increase in tumors, and it probably was because of the abnormal energy metabolism during exacerbation. This data further indicated the reliability of our sensor used under a hypoxic tumor microenvironment.

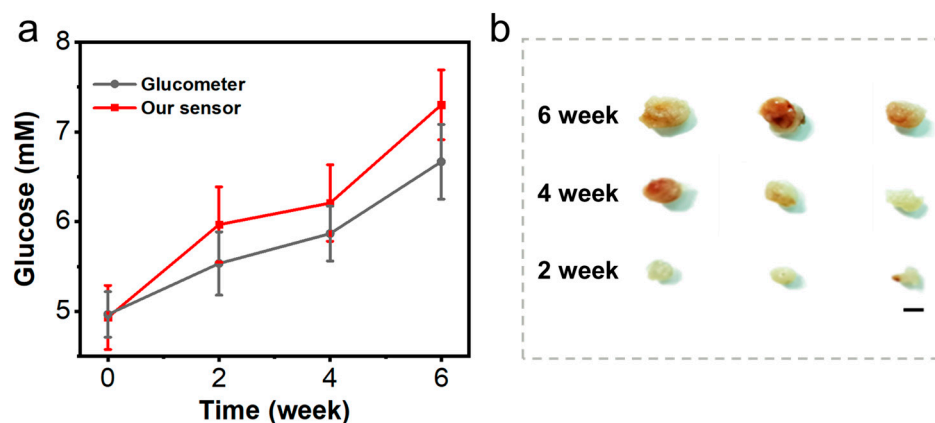


**Figure 6.** (a) Glucose levels measured in the ISF surrounding the hypoxic microenvironment of tumor tissue in the tumor-bearing mice using our sensor versus that using the reference glucometer. (b) Photographs of excised tumors. The black line in (b) represent the scale bar (3 mm).

#### 4. Conclusions

Glucose monitoring is important for the glucose management of diabetics. However, most common glucose sensors are dependent on enzymes and oxygen for the detection reaction, which may lead to biased results due to the reduction of enzyme activity and fluctuation of oxygen in tissues. Hence, development of a kind of glucose sensor that does not rely on enzymes and oxygen are highly anticipated.

In this work, we developed a nonenzymatic glucose sensor based on WSE for CGM under hypoxic microenvironment. Since the WSE reaction did not require the participation of oxygen, our nonenzymatic glucose sensor was not affected by the oxygen. Moreover, the stability and accuracy of our sensor were confirmed by the *in vivo* and *in vitro* tests. The test results indicated that our designed sensor had acceptable sensitivity, selectivity, reproducibility, stability for CGM *in vivo* and *in vitro*, especially under hypoxic environments. Moreover, in contrast to the conventional enzyme-based sensors, which are vulnerable due to decreased enzyme activity and changing physiological conditions, our nonenzymatic sensor was robust and stable. These features indicated that our designed nonenzymatic CGM sensor is a promising glucose sensor for diabetes management and clinical applications in hypoxic microenvironments.

Although the function and the reliability of our proposed nonenzymatic CGM sensor have been demonstrated, this sensor is still of some limitation, which needs to be addressed before its real-world application. In this work, we used a hard glass tube for the fabrication of the sensor, which needs to be replaced with a softer and more flexible material such as polydimethylsiloxane to improve comfort and reduce the pain for long-term glucose monitoring in practical application. Moreover, some engineering work to reduce the sensor size and integrate our sensor with smartphones via wireless connection to improve its portability is worth considering. Finally, further research and more tests to prove the reliability, safety, and function of the sensor for large-scale application is highly required.

**Supplementary Materials:** The following supporting information can be downloaded at: <https://www.mdpi.com/article/10.3390/chemosensors11020149/s1>. Figure S1: micrographs of (a) the three-hole glass capillary and (b) the capillary with three electrodes; Figure S2: (a) potential of the Au electrode as a function of time used to determine the pH value on the electrode surface, (b) potential measured in 200 s as a function of the pH of the solution, (c) pH measured on the gold electrode surface as a function of pretreatment ( $-2.0$  V) time; Figure S3: amperometric responses for glucose determination obtained in artificial ISF containing 5.0 mM glucose and interfering substances; Figure S4: results of the replicated tests in an artificial ISF containing 5.0 mM glucose for 10 times; Figure S5: results of replicated tests in an artificial ISF containing 5.0 mM glucose during 30 days; Figure S6: dissolved oxygen levels in artificial ISF as a function of nitrogen purging time (flow rate: 10 mL/s);

Figure S7: results of fasting glucose detection using our sensor versus CGM-2 sensor in a rat during 16 days.

**Author Contributions:** Conceptualization, C.Z., and H.L.; Formal analysis, L.L., C.X., X.D., B.M., Y.C., and Q.H.; Funding acquisition, B.M., Q.H., C.Z., and H.L.; Investigation, L.L., C.X., X.D., B.M., and Y.C.; Methodology, L.L., C.Z., and H.L.; Project administration, H.L.; Validation, L.L., X.D., and H.L.; Writing—original draft, L.L.; Writing—review & editing, B.M., Q.H., C.Z., and H.L. All authors have read and agreed to the published version of the manuscript.

**Funding:** This work was supported by the Key Research and Development Program of Jiangsu Province (BE2021700), National Natural Science Foundation of China (62001104, 62271136), National Key Research and Development Plan (2022YFF1201803, 2021YFB2600800), Natural Science Foundation of Jiangsu Province (BK20200357), Science and Technology Development Program of Suzhou (SYG202117), Key Project and Open Research Fund of State Key Laboratory of Bioelectronics, the Fundamental Research Funds for the Central Universities (2242022R10052), and Zhishan Young Scholars of Southeast University (2242022R40017).

**Institutional Review Board Statement:** Not applicable.

**Informed Consent Statement:** Not applicable.

**Data Availability Statement:** Not applicable.

**Conflicts of Interest:** The authors declare no conflict of interest.

## References

1. Teymourian, H.; Barfidokht, A.; Wang, J. Electrochemical glucose sensors in diabetes management: An updated review (2010–2020). *Chem. Soc. Rev.* **2020**, *49*, 7671–7709. [[CrossRef](#)] [[PubMed](#)]
2. Lee, I.; Probst, D.; Klonoff, D.; Sode, K. Continuous glucose monitoring systems—Current status and future perspectives of the flagship technologies in biosensor research. *Biosens. Bioelectron.* **2021**, *181*, 113054. [[CrossRef](#)] [[PubMed](#)]
3. Mahmoudi, Z.; Del Favero, S.; Jacob, P.; Choudhary, P.; Hypo, R.C. Toward an optimal definition of hypoglycemia with continuous glucose monitoring. *Comput. Methods Programs Biomed.* **2021**, *209*, 106303. [[CrossRef](#)] [[PubMed](#)]
4. Lin, R.; Brown, F.; Ekinci, E.I. The ambulatory glucose profile and its interpretation. *Med. J. Aust.* **2022**, *217*, 295–298. [[CrossRef](#)] [[PubMed](#)]
5. Ghadiya, S.; Jain, A.; Pandya, H.; Lakhani, J.D. Continuous blood glucose monitoring to determine the glycemic variability in patients having SARS CoV-2 infection with ARDS and its bearing on the severity of the disease. *J. Adv. Med. Med. Res.* **2020**, *116*, 51–56. [[CrossRef](#)]
6. Bando, H.; Ebe, K.; Muneta, T.; Bando, M.; Yonei, Y. Detail glucose fluctuation and variability by continuous glucose monitoring (CGM). *J. Diabetes Metab. Disord. Control* **2020**, *7*, 31–35. [[CrossRef](#)]
7. Lee, H.; Hong, Y.J.; Baik, S.; Hyeon, T.; Kim, D.H. Enzyme-based glucose sensor: From invasive to wearable device. *Adv. Healthc. Mater.* **2018**, *7*, e1701150. [[CrossRef](#)]
8. DeHennis, A.; Mortellaro, M. CGM sensor technology. In *Glucose Monitoring Devices*; Academic Press: Cambridge, MA, USA, 2020; pp. 111–134. [[CrossRef](#)]
9. Lim, S.; Bae, J.H.; Kwon, H.S.; Nauck, M.A. COVID-19 and diabetes mellitus: From pathophysiology to clinical management. *Nat. Rev. Endocrinol.* **2021**, *17*, 11–30. [[CrossRef](#)]
10. Velavan, T.P.; Meyer, C.G. The COVID-19 epidemic. *Trop. Med. Int. Health* **2020**, *25*, 278–280. [[CrossRef](#)] [[PubMed](#)]
11. Felsenstein, S.; Herbert, J.A.; McNamara, P.S.; Hedrich, C.M. COVID-19: Immunology and treatment options. *Immunol. Treat. Options* **2020**, *215*, 108448. [[CrossRef](#)]
12. Bein, T.; Grasso, S.; Moerer, O.; Quintel, M.; Guerin, C.; Deja, M.; Brondani, A.; Mehta, S. The standard of care of patients with ARDS: Ventilatory settings and rescue therapies for refractory hypoxemia. *Intensive Care Med.* **2016**, *42*, 699–711. [[CrossRef](#)]
13. Mistry, N.; Mazer, C.D.; Sled, J.G.; Lazarus, A.H.; Cahill, L.S.; Solish, M.; Zhou, Y.Q.; Romanova, N.; Hare, A.G.M.; Doctor, A.; et al. Red blood cell antibody-induced anemia causes differential degrees of tissue hypoxia in kidney and brain. *J. Physiol.-Regul. Integr. Comp. Physiol.* **2018**, *314*, R611–R622. [[CrossRef](#)]
14. Siwaponanan, P.; Fucharoen, S.; Sirankapracha, P.; Winichagoon, P.; Umemura, T.; Svasti, S. Elevated levels of miR-210 correlate with anemia in beta-thalassemia/HbE patients. *Int. J. Hematol.* **2016**, *104*, 338–343. [[CrossRef](#)] [[PubMed](#)]
15. He, L.N.; Chen, W.; Yang, Y.; Xie, Y.J.; Xiong, Z.Y.; Chen, D.Y.; Lu, D.; Liu, N.Q.; Yang, Y.H.; Sun, X.F. Elevated prevalence of abnormal glucose metabolism and other endocrine disorders in patients with beta-thalassemia major: A meta-analysis. *BioMed Res. Int.* **2019**, *2019*, 6573497. [[CrossRef](#)] [[PubMed](#)]
16. Soliman, A.T.; Yasin, M.; El-Awwa, A.; De Sanctis, V. Detection of glycemic abnormalities in adolescents with beta thalassemia using continuous glucose monitoring and oral glucose tolerance in adolescents and young adults with beta-thalassemia major: Pilot study. *Indian J. Endocrinol. Metab.* **2013**, *17*, 490–495. [[CrossRef](#)] [[PubMed](#)]

17. Zeng, W.; Liu, P.; Pan, W.; Singh, S.R.; Wei, Y. Hypoxia and hypoxia inducible factors in tumor metabolism. *Cancer Lett.* **2015**, *356*, 263–267. [[CrossRef](#)] [[PubMed](#)]
18. Mao, L. Electrochemical Sensors Dancing with the Brain. *ACS Sens.* **2020**, *5*, 2659–2660. [[CrossRef](#)]
19. Chen, C.; Xie, Q.; Yang, D.; Xiao, H.; Fu, Y.; Tan, Y.; Yao, S. Recent advances in electrochemical glucose biosensors: A review. *RSC Adv.* **2013**, *3*, 4473–4491. [[CrossRef](#)]
20. Feldman, B.; Brazg, R.; Schwartz, S.; Weinstein, R. A continuous glucose sensor based on wired enzyme technology—Results from a 3-day trial in patients with type 1 diabetes. *Diabetes Technol. Ther.* **2003**, *5*, 769–779. [[CrossRef](#)]
21. Harris, J.M.; Reyes, C.; Lopez, G.P. Common causes of glucose oxidase instability in in vivo biosensing: A brief review. *J. Diabetes Sci. Technol.* **2013**, *7*, 1030–1038. [[CrossRef](#)]
22. Anwar, S.; Khan, F.; Zhang, Y.; Djire, A. Recent development in electrocatalysts for hydrogen production through water electrolysis. *Int. J. Hydrog. Energy* **2021**, *46*, 32284–32317. [[CrossRef](#)]
23. Tian, L.; Li, Z.; Xu, X.; Zhang, C. Advances in noble metal (Ru, Rh, and Ir) doping for boosting water splitting electrocatalysis. *J. Mater. Chem. A* **2021**, *9*, 13459–13470. [[CrossRef](#)]
24. Anantharaj, S.; Ede, S.R.; Sakthikumar, K.; Karthick, K.; Mishra, S.; Kundu, S. Recent trends and perspectives in electrochemical water splitting with an emphasis on sulfide, selenide, and phosphide catalysts of Fe, Co, and Ni: A review. *Acs Catal.* **2016**, *6*, 8069–8097. [[CrossRef](#)]
25. Bollella, P.; Sharma, S.; Cass, A.E.G.; Antiochia, R. Minimally-invasive microneedle-based biosensor array for simultaneous lactate and glucose monitoring in artificial interstitial fluid. *Electroanalysis* **2019**, *31*, 374–382. [[CrossRef](#)]
26. Fang, Y.; Wang, S.; Liu, Y.; Xu, Z.; Zhang, K.; Guo, Y. Development of Cu nanoflowers modified the flexible needle-type microelectrode and its application in continuous monitoring glucose in vivo. *Biosens. Bioelectron.* **2018**, *110*, 44–51. [[CrossRef](#)]
27. Lu, X.; Qin, L.; Guo, M.; Geng, J.; Dong, S.; Wang, K.; Xu, H.; Qu, C.; Miao, J.; Liu, M. A novel alginate from Sargassum seaweed promotes diabetic wound healing by regulating oxidative stress and angiogenesis. *Carbohydr. Polym.* **2022**, *289*, 119437. [[CrossRef](#)]
28. Song, X.; Feng, L.; Liang, C.; Yang, K.; Liu, Z. Ultrasound triggered tumor oxygenation with oxygen-shuttle nanoporous carbon to overcome hypoxia-associated resistance in cancer therapies. *Nano Lett.* **2016**, *16*, 6145–6153. [[CrossRef](#)]
29. Wen, Y.; Wang, X.; Cai, P.; Yu, X. Application of a platinum sheet for pH measurement based on chronopotentiometry. *Sens. Actuators B Chem.* **2015**, *216*, 409–411. [[CrossRef](#)]
30. Lei, L.; Zhao, C.; Zhu, X.; Yuan, S.; Dong, X.; Zuo, Y.; Liu, H. Nonenzymatic electrochemical sensor for wearable interstitial fluid glucose monitoring. *Electroanalysis* **2022**, *34*, 415–422. [[CrossRef](#)]
31. Park, S.; Boo, H.; Chung, T.D. Electrochemical non-enzymatic glucose sensors. *Anal. Chim. Acta* **2006**, *556*, 46–57. [[CrossRef](#)]
32. Lorenz, C.; Sandoval, W.; Mortellaro, M. Interference assessment of various endogenous and exogenous substances on the performance of the eversense long-term implantable continuous glucose monitoring system. *Diabetes Technol. Ther.* **2018**, *20*, 344–352. [[CrossRef](#)]
33. Tang, L.; Cui, T.; Wu, J.J.; Liu-Mares, W.; Huang, N.; Li, J. A rice-derived recombinant human lactoferrin stimulates fibroblast proliferation, migration, and sustains cell survival. *Wound Repair Regen.* **2010**, *18*, 123–131. [[CrossRef](#)] [[PubMed](#)]
34. Cai, L.; Qin, X.; Xu, Z.; Song, Y.; Jiang, H.; Wu, Y.; Ruan, H.; Chen, J. Comparison of cytotoxicity evaluation of anticancer drugs between real-time cell analysis and CCK-8 method. *Acs Omega* **2019**, *4*, 12036–12042. [[CrossRef](#)] [[PubMed](#)]
35. Tang, Z.; Louie, R.F.; Lee, J.H.; Lee, D.M.; Miller, E.E.; Kost, G.J. Oxygen effects on glucose meter measurements with glucose dehydrogenase- and oxidase-based test strips for point-of-care testing. *Crit. Care Med.* **2001**, *29*, 1062–1070. [[CrossRef](#)] [[PubMed](#)]
36. Lv, J.; Liang, Y.; Tu, Y.; Chen, J.; Xie, Y. Hypoxic preconditioning reduces propofol-induced neuroapoptosis via regulation of Bcl-2 and Bax and downregulation of activated caspase-3 in the hippocampus of neonatal rats. *Neurol. Res.* **2018**, *40*, 767–773. [[CrossRef](#)] [[PubMed](#)]
37. Stetler, R.A.; Leak, R.K.; Gan, Y.; Li, P.; Zhang, F.; Hu, X.; Jing, Z.; Chen, J.; Zigmond, M.J.; Gao, Y. Preconditioning provides neuroprotection in models of CNS disease: Paradigms and clinical significance. *Prog. Neurobiol.* **2014**, *114*, 58–83. [[CrossRef](#)] [[PubMed](#)]
38. Wee, J.; Climstein, M. Hypoxic training: Clinical benefits on cardiometabolic risk factors. *J. Sci. Med. Sport* **2015**, *18*, 56–61. [[CrossRef](#)]
39. Gerber, P.A.; Rutter, G.A. The role of oxidative stress and hypoxia in pancreatic beta-cell dysfunction in diabetes mellitus. *Antioxid. Redox Signal.* **2017**, *26*, 501–518. [[CrossRef](#)]

**Disclaimer/Publisher’s Note:** The statements, opinions and data contained in all publications are solely those of the individual author(s) and contributor(s) and not of MDPI and/or the editor(s). MDPI and/or the editor(s) disclaim responsibility for any injury to people or property resulting from any ideas, methods, instructions or products referred to in the content.